

Performance Analysis of Ultra-Wideband Spatial MIMO Communications Systems

Wasim Q. Malik, Matthews C. Mtumbuka, David J. Edwards, Christopher J. Stevens
Department of Engineering Science, University of Oxford, Parks Road, Oxford OX1 3PJ, U.K.
{wasim.malik, matthews.mtumbuka, david.edwards, christopher.stevens}@eng.ox.ac.uk

Abstract—The performance of an ultra-wideband multiple-input-multiple-output (MIMO) communications system is experimentally evaluated. Using 3x3 indoor channel measurements, it is demonstrated that the MIMO subchannels are highly uncorrelated, with correlation coefficients lower than 0.45. Eigenvalue decomposition further confirms the channel independence. A linear gain in outage capacity is demonstrated. A spectral efficiency of 15.5 b/s/Hz is obtained, compared to 3 b/s/Hz for narrowband SISO. Thus a full-band tri-element UWB system can yield a 1% outage capacity of up to 184.5 Gbps.

Keywords—Capacity, correlation, MIMO, multiple antenna, spectral efficiency, ultra-wideband (UWB).

I. INTRODUCTION

Ultra-wideband (UWB) is a rapidly emerging communications technique that uses a very large spreading bandwidth B , resulting in a large Shannon capacity and high data rate [1-3]. For a UWB system, the bandwidth is greater than the channel coherence bandwidth, inducing frequency-selectivity to the system. A large number of incoming multipath components are temporally resolved [4] as a consequence of frequency selectivity [5] and high time resolution. The power delay profiles (PDPs) are thus uncorrelated even for small receiver displacements, which is promising for the performance advantage of diversity and MIMO systems.

Multiple-input-multiple-output (MIMO) is a multiple antenna technique that, under the condition of orthogonal signal propagation, increases the information theoretic channel capacity linearly with the number of antenna elements [6-10]. MIMO systems exploit signal orthogonality to create a set of parallel subchannels through the use of antenna arrays at transmitter and receiver. This is especially effective in scattering environments, such as wideband and non-line-of-sight channels, that have low spatial correlation [11].

UWB and MIMO are techniques that enhance the information capacity and spectral efficiency of the channel respectively. As UWB uses microwave frequencies in the 3.1–10.6 GHz range [12], the antenna element separation required for signal orthogonality is small. This enables high device integration and compact systems that provide very high data rates. A multiple-antenna UWB communications system is thus a leading candidate for future wireless communications systems supporting gigabit capacities. Early results with MIMO using three-branch polarization on UWB channels

show achievable Shannon capacities of over 150 Gbps [13]. This is a consequence of the high spectral efficiency provided by MIMO over the large bandwidth of the UWB system.

In this paper, we evaluate the performance of UWB MIMO systems using spatial orthogonality. We examine the correlation properties of the 3x3 UWB-MIMO channel. We evaluate the increase in system capacity, which is expected to be three times that of a single UWB link and many orders higher than a narrowband link. We also analyze the variation of the correlation coefficient with frequency, which gives an insight into the frequency bands most suitable for UWB-MIMO operation with the antenna configuration and separation used in the experiment.

II. MEASUREMENT CONFIGURATION

Our analysis is based on channel measurements carried out in an indoor environment using a vector network analyzer (VNA) measurement system [14]. A plan representation of the measurement environment is shown in Fig. 1.

Two identical omni-directional discone antennas connected to the input and output ports of the VNA are used for channel sounding in the UWB frequency band (3.1–10.6 GHz), so that $B = 7.5$ GHz. As a 3x3 MIMO system is studied, therefore $n_t = n_r = 3$. The three transmitting antennas are placed linearly, 0.06 m apart. In order to prevent antenna coupling from affecting the measurement results, the measurements from the three antenna positions are carried out sequentially instead of simultaneously, assuming a quasi-static indoor channel.

A large aluminium sheet is placed between the transmitter and receiver to create a non-line-of-sight (NLOS) scenario, while there is a clear direct path in the LOS measurement. A 30 dB low-noise amplifier is used at the receiver, and the overall measurement system is calibrated to remove frequency-dependent attenuation and phase distortion.

For each transmitter location, the received complex signal is measured using a computer-controlled 30x30 Cartesian measurement grid with a resolution of $\Delta_d = 0.03$ m. This is then used to generate MIMO transfer functions for each of the subchannels such that both the transmitter and the receiver antenna elements are 0.06 m apart (measured from the outer surface of the antennas). The complex transfer functions are recorded by sounding the channel at $n_f = 1601$ discrete frequencies, such that the frequency resolution of the measurement $\Delta_f = B / (n_f - 1) = 4.7$ MHz. This resolution is

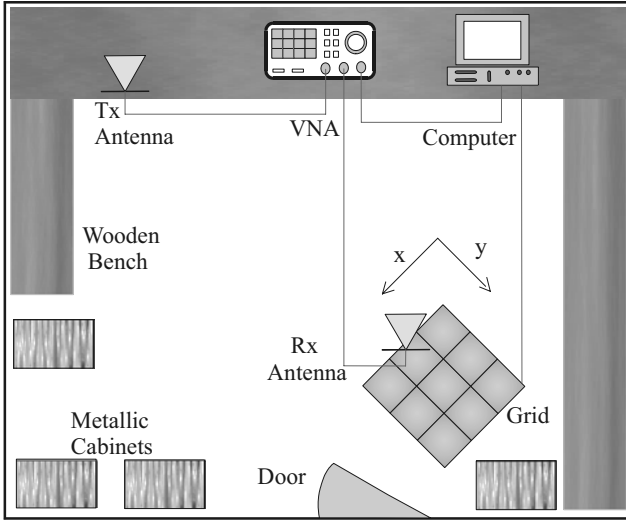


Fig. 1. Indoor MIMO channel measurement system

also approximately equal to the multiband orthogonal frequency division multiplexing (MB-OFDM) implementation of UWB and the analysis is therefore especially useful for such systems.

III. MIMO CHANNEL FORMULATION

For each measurement point, the complex transfer function

$$G_{x,y,f} = \alpha_{x,y,f} e^{j\phi_{x,y,f}}, \quad x, y \in \{1, \dots, n_d\}, f \in \{1, \dots, n_f\} \quad (1)$$

is logged, where $\alpha_{x,y,f}$ and $\phi_{x,y,f}$ are the measured magnitude and phase responses at frequency f on grid position (x, y) . It is then power-normalized to remove the effect of pathloss from influencing the result, i.e.

$$H_{x,y,f} = \frac{G_{x,y,f}}{\sqrt{\sum_{f=1}^{n_f} |G_{x,y,f}|^2}} = \frac{G_{x,y,f}}{\sqrt{\sum_{f=1}^{n_f} \alpha_{x,y,f}^2}}. \quad (2)$$

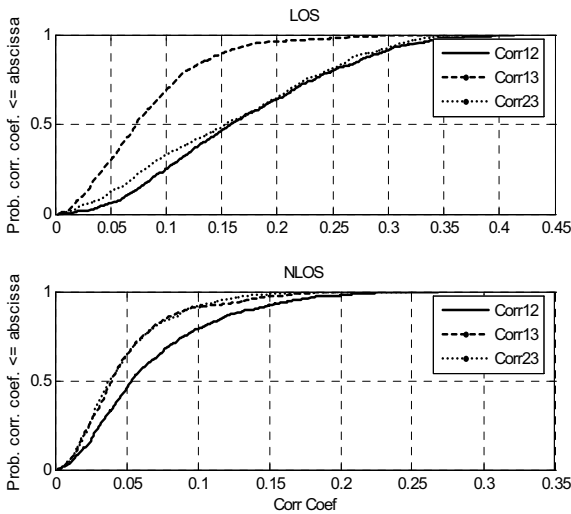


Fig. 2. Cumulative distribution function of transmit correlation

The MIMO channel matrix $\mathbf{H} \in \mathbb{C}^{n_T \times n_R \times n_f}$ is formed by collating the normalized transfer functions of all the subchannels, where n_T and n_R denote the number of transmit and receive antennas respectively:

$$\mathbf{H} = [H_{TR,f}], \quad T, R \in \{1, 2, 3\}, f \in [f_l, f_h]. \quad (3)$$

IV. CORRELATION ANALYSIS

A well-established criterion for the evaluation of MIMO performance is the decorrelation of the individual subchannels [15]. This can be determined from correlation analysis. The correlation between two random variables x and y is defined by

$$r_{xy} = \frac{E[xy] - E[x]E[y]}{\sqrt{(E[x^2] - E[x]^2)(E[y^2] - E[y]^2)}} \quad (4)$$

where $E[\cdot]$ represents expectation. The correlation between the elements of the measured MIMO channel matrix \mathbf{H} is calculated. We calculate the receive correlation ρ_{R1-R2} between the signals transmitted by antenna T_1 and received by receivers R_1 and R_2 . Similarly the transmit correlation is also calculated. This is carried out for all combination of the transmitting and receiving antenna elements. Fig. 2 shows the cumulative distribution functions (CDFs) of the transmit correlation coefficients for LOS and NLOS. It is found that ρ is less than 0.45 and 0.3 for the LOS and NLOS propagation conditions respectively. The correlation between antennas 1 and 3 is generally lower than the other two combinations because of the greater separation. Similarly, Fig. 3 shows the receive correlation for LOS and NLOS, which is found to have slightly higher values in general. The results are summarized in Tables I and II.

Noting that the spatial correlation is a function of antenna separation in terms of wavelength, we also study the variation in correlation with frequency, shown in Fig. 4. The transmit correlation is found to have a mean value of about 0.15 across the spectrum, though in the LOS case the transmit correlation is significantly high in the 7–8 GHz band. The receive correlation also varies with frequency, as shown in Fig. 5, with

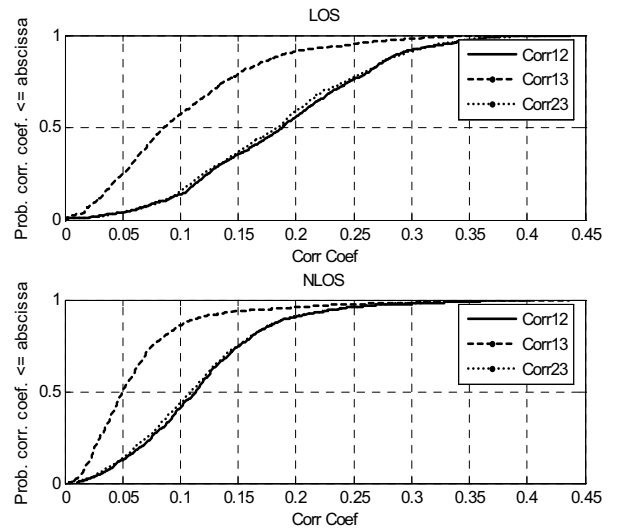


Fig. 3. Cumulative distribution function of receive correlation

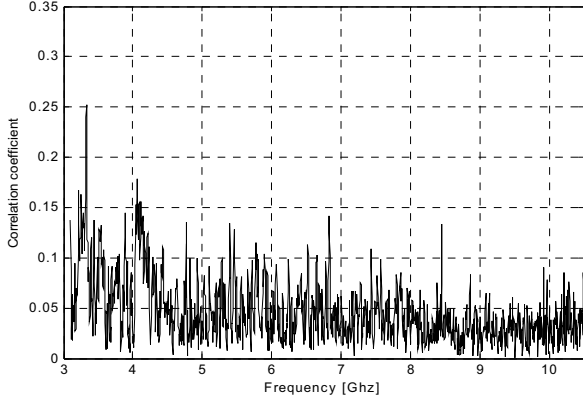


Fig. 4. Transmit correlation as a function of frequency

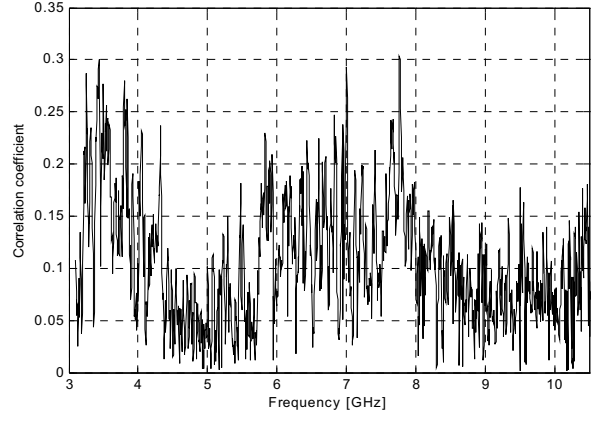


Fig. 5. Receive correlation as a function of frequency

the highest value of the correlation coefficient obtained near the lower end of the band. Both transmit and receive correlations show an approximately oscillatory behavior in the LOS situation, but no pattern is found in the NLOS case. This information can be used to identify the optimal sub-bands for a multiband UWB-MIMO system.

V. EIGENVALUE DECOMPOSITION

Eigenvalue decomposition is also used to determine the number of orthogonal sub-channels. The eigenvalues λ_i , $i=\{1, \dots, k\}$, of the correlation matrix

$$\mathbf{R} = \mathbf{H}\mathbf{H}^H \quad (5)$$

represent the power gains of the k orthogonal subchannels [9], where the notation $(.)^H$ signified the Hermitian transpose. Fig. 6 shows the CDFs of the LOS and NLOS eigenvalues. The clear separation of the eigenvalue CDF curves indicates that the three orthogonal subchannels can be used for independent transmission of data thereby increasing the capacity of both LOS and NLOS UWB channels. Significant diversity gain is also achieved through this system, as obvious from the

eigenvalue separation.

Further evidence of the existence of three effective degrees of freedom in the analyzed UWB MIMO system is obtained from the fact that the channel matrix \mathbf{H} has full rank. This confirms that the indoor UWB channel can be decomposed into three independent spatial sub-channels.

Singular value decomposition (SVD) can be used to decompose the channel matrix \mathbf{H} into a diagonal matrices that contains the eigenvalues of \mathbf{R} and two unitary matrices that specify the optimal weights for transmit and receive antennas for water-filling power allocation in the presence of channel state information (CSI) at both transmitter and receiver. However, that analysis is beyond the scope of the current paper and will not be pursued here.

VI. MIMO CAPACITY

The cumulative distribution function (CDF) of spectral efficiency C , where

TABLE I MAXIMUM TRANSMIT CORRELATION		
Channels	LOS	NLOS
1 and 2	0.41	0.27
2 and 3	0.39	0.25
1 and 3	0.40	0.20

TABLE II MAXIMUM RECEIVE CORRELATION		
Channels	LOS	NLOS
1 and 2	0.44	0.40
2 and 3	0.42	0.40
1 and 3	0.41	0.44

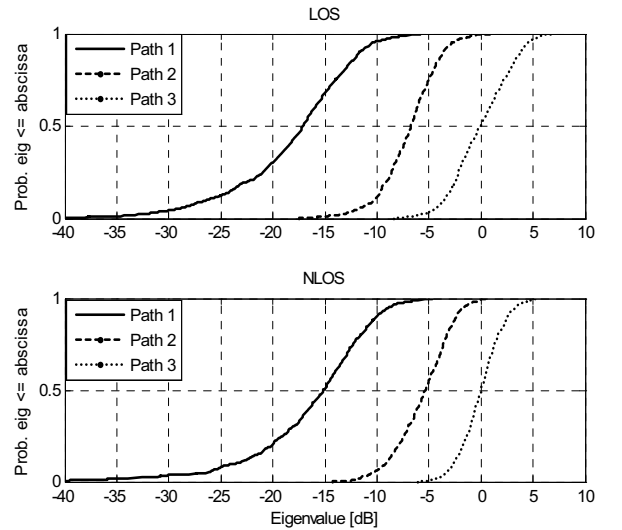


Fig. 6. Eigenvalue decomposition

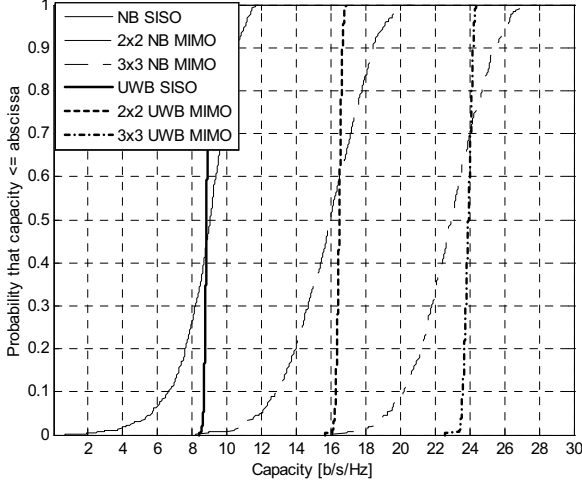


Fig.7. Spectral efficiency (LOS)

$$C = \frac{1}{B} \sum_{f=1}^{n_f} \log_2 \left| I + \frac{\gamma}{n_t} H^H H \right| \Delta f, \quad (6)$$

is obtained, where it is assumed that the SNR γ is 30 dB. Here $(\cdot)^H$ denotes the Hermitian transpose of a matrix.

Fig. 7 and 8 show the CDFs of C for narrowband (NB) and UWB systems with single-input-single-output (SISO) and MIMO configurations in the LOS and NLOS environments respectively. $C_{NB-SISO}$ and $C_{NB-MIMO}$ are calculated for the case of a single discrete frequency at the centre of the UWB band, i.e. at 6.85 GHz. Diversity and MIMO performance is typically analyzed at an outage probability of 1% or 10%, as higher outage probabilities render a system unreliable and thus of limited use. At these values, the MIMO CDF curves yield considerably higher spectral efficiencies than the corresponding SISO configurations. Tables III and IV show the mean capacities for both the LOS and NLOS cases. It can be observed that $C_{UWB-MIMO} = 23.9$ b/s/Hz, which is an increase of

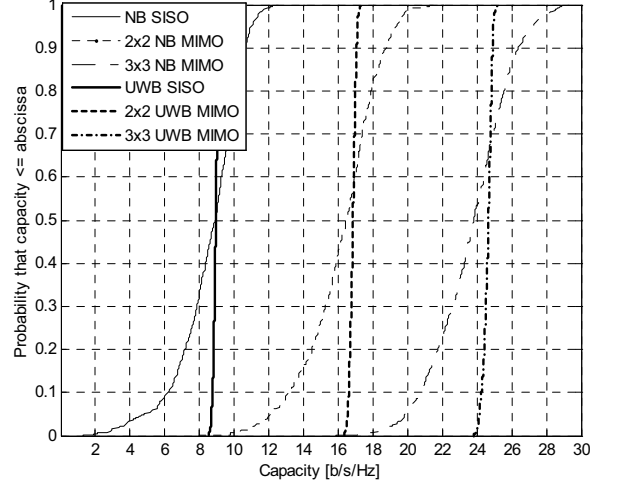


Fig.8. Spectral efficiency (NLOS)

15.7 b/s/Hz from $C_{NB-SISO}$. Even higher capacities are obtained in the NLOS channel, where $C_{UWB-MIMO} = 24.6$ b/s/Hz. In both LOS and NLOS, the capacity increases almost linearly with the number of antenna elements for narrowband and UWB channels. This confirms that the use of additional antenna elements in a MIMO configuration provides similar increase in capacity in UWB as has been earlier demonstrated for narrowband systems.

It can also be observed that the spectral efficiency CDFs for UWB-SISO and UWB-MIMO are much steeper than their narrowband counterparts. This confirms that a UWB channel is much more stable than a narrowband channel, due to its resistance to small-scale fading [1]. It has been shown previously that in wideband frequency-selective channels, the outage capacity approaches the mean capacity [15]. Our results indicate that UWB also follows this behavior, and the variance of capacity is low due to reduced fading in the UWB channel.

For a UWB system using a 7.5 GHz bandwidth with 3x3 MIMO, this value of C corresponds to a capacity of 184.5 Gbps at a 30 dB SNR. Such high throughputs are unprecedented in radio communications and cannot be achieved with conventional techniques. Furthermore, this capacity is achieved with linearly arranged antennas covering only a small area, since our analysis uses a spatial separation of 6 cm between adjacent antennas. Using this technique, almost 200 individual gigabit wireless links can be supported within a cell of a few meters radius with very high quality of service (QoS).

VII. CONCLUSION

The performance of 3x3 spatial UWB-MIMO has been numerically evaluated in this paper using indoor channel measurements. A high degree of signal decorrelation is observed for all frequencies within the band for both LOS and NLOS scenarios. The correlation coefficients are lower than 0.45 for a linear antenna separation of 6 cm. Three distinct eigenvalues are obtained, confirming the subchannel orthogonality. It is found that the outage capacity has a value

TABLE III
MEAN CAPACITY – LOS

Antenna Elements	Narrowband	Ultra-Wideband
1x1 SISO	8.2	8.8
2x2 MIMO	15.8	16.5
3x3 MIMO	22.9	23.9

TABLE IV
MEAN CAPACITY – NLOS

Antenna Elements	Narrowband	Ultra-Wideband
1x1 SISO	8.6	8.9
2x2 MIMO	16.2	16.8
3x3 MIMO	23.7	24.6

close to the mean capacity in the UWB channel, i.e. there is much less variation in capacity. A linear increase in spectral efficiency with the number of antenna elements is observed. At a 1% outage probability, a spectral efficiency of up to 24.6 b/s/Hz can be achieved with this technique. For a full-band UWB-MIMO link operating at 30 dB SNR (in short range communication), system capacities as high as 184.5 Gbps can be obtained.

REFERENCES

- [1] M. Z. Win and R. A. Scholtz, "Characterization of ultra-wideband wireless indoor channels: a communication-theoretic view," *IEEE J. Select. Areas Commun.*, vol. 20, December 2002.
- [2] S. S. Ghassemzadeh, R. Jana, C. W. Rice, W. Turin, and V. Tarokh, "Measurement and modeling of an ultra-wide bandwidth indoor channel," *IEEE Trans. Commun.*, vol. 52, October 2004.
- [3] R. J.-M. Cramer, R. A. Scholtz, and M. Z. Win, "An evaluation of the ultra-wideband propagation channel," *IEEE Transactions on Antennas and Propagation*, vol. 50, May 2002.
- [4] W. Q. Malik, D. J. Edwards, and C. J. Stevens, "Experimental evaluation of Rake receiver performance in a line-of-sight ultra-wideband channel," in *Proc. Joint IEEE UWBST & IWUWBS*. Kyoto, Japan, 18-21 May 2004.
- [5] W. Q. Malik, D. J. Edwards, and C. J. Stevens, "Small-scale delay-domain statistics of the frequency-selective indoor wireless channel," in *Proc. IEEE INMIC*. Lahore, Pakistan, December 2004 (In press).
- [6] J. H. Winters, "On the capacity of radio communications systems with diversity in Rayleigh fading environments," *IEEE J. Select. Areas Commun.*, vol. 5, June 1987.
- [7] G. J. Foschini and M. J. Gans, "On limits of wireless communications in a fading environment when using multiple antennas," in *Wireless Personal Commun.*, vol. 6: Kluwer Academic Press, March 1998.
- [8] I. E. Telatar, "Capacity of multi-antenna Gaussian channels," *European Transactions on Telecommunications*, vol. 10, November/December 1999.
- [9] J. B. Andersen, "Array gain and capacity for known random channels with multiple element arrays at both ends," *IEEE J. Select. Areas Commun.*, vol. 18, November 2000.
- [10] M. C. Mtumbuka and D. J. Edwards, "Investigation of a tri-polarized MIMO technique," *Electron. Lett.*, (in press).
- [11] P. F. Driessen and G. J. Foschini, "On the capacity formula for multiple input-multiple output wireless channels: a geometric interpretation," *IEEE Trans. Commun.*, vol. 47, February 1999.
- [12] "Revision of Part 15 of the Commission's rules regarding ultra-wideband transmission systems: First report and order," Federal Communications Commission, Washington, DC, USA FCC 02-48, 14 February 2002.
- [13] M. C. Mtumbuka, W. Q. Malik, C. J. Stevens, and D. J. Edwards, "A tri-polarized ultra-wideband MIMO system," in *Proc. IEEE Sarnoff Symp.* Princeton, NJ, USA, April 2005 (in press).
- [14] A. M. Street, L. Lukama, and D. J. Edwards, "On the use of VNAs for wideband propagation measurements," *IEE Proc.-Commun.*, vol. 148, December 2001.
- [15] A. F. Molisch, M. Steinbauer, M. Toeltsch, E. Bonek, and R. S. Thomä, "Capacity of MIMO systems based on measured wireless channels," *IEEE J. Select. Areas Commun.*, vol. 20, April 2002.